Princeton Plasma Physics Laboratory

PPPL- 5047

PPPL- 5047

Phase-locking of Magnetic Islands Diagnosed by ECE-Imaging

B. Tobias, B.A. Grierson, C.M. Muscatello, X. Ren, C.W. Domier, N.C. Luhmann, Jr., S.E. Zemedkun, T.L. Munsat, and I.G.J. Classen

June 2014

PPPL PRINCETON PLASMA PHYSICS LABORATORY

Prepared for the U.S. Department of Energy under Contract DE-AC02-09CH11466.

Princeton Plasma Physics Laboratory
Report Disclaimers

Full Legal Disclaimer

Trademark Disclaimer

PPPL Report Availability

Princeton Plasma Physics Laboratory:

http://www.pppl.gov/techreports.cfm

Office of Scientific and Technical Information (OSTI):

http://www.osti.gov/scitech/

Related Links:

U.S. Department of Energy

Office of Scientific and Technical Information

Phase-locking of magnetic islands diagnosed by ECE-Imaging[a)]

B. Tobias[1,b], B.A. Grierson[1], C.M. Muscatello[2], X. Ren[2], C.W. Domier[2], N.C. Luhmann, Jr.[2], S.E. Zemedkun[3], T.L. Munsat[3], and I.G.J. Classen[4]
[1]*Princeton Plasma Physics Laboratory, Princeton, NJ 08543, USA*
[2]*Universtiy of California at Davis, Davis, CA 95616, USA*
[3]*University of Colorado at Boulder, Boulder, CO 80309, USA*
[4]*Dutch Institute for Fundamental Energy Research-DIFFER, 3430 BE Nieuwegein, The Netherlands*

(Presented XXXXX; received XXXXX; accepted XXXXX; published online XXXXX)

Millimeter-wave imaging diagnostics identify phase-locking and the satisfaction of 3-wave coupling selection criteria amongst multiple magnetic island chains by providing a localized, internal measurement of the 2D power spectral density, $S(\omega,k_{pol})$. In high-confinement tokamak discharges, these interactions impact both plasma rotation and tearing stability. Nonlinear coupling amongst neoclassical tearing modes (NTMs) of different *n*-number, with islands not satisfying the poloidal mode number selection criterion $\langle m,m',m-m'\rangle$, contributes to a reduction in core rotation and flow shear in the vicinity of the modes.

I. INTRODUCTION

Linear, electromagnetic coupling due to toroidicity (toroidal coupling) and the subsequent phase-locking of two tearing modes has often been indicated in seed island destabilization of potentially dangerous NTMs[1-3], and tearing stability in general[4,5]. For modes of like *n*-number, $J\times B$ forces arise in the overlap of $m\pm1$ sidebands inherent to each magnetic island. However, toroidal coupling does not account for the coupling of modes having different toroidal mode number, *n*, which remains a good quantum number in axisymmetric toroidal geometry. In these scenarios, nonlinear 3-wave coupling dominates for modes satisfying the selection criteria $\langle k,k',k-k'\rangle$ and $\langle\omega,\omega',\omega-\omega'\rangle$. This has been described analytically for cylindrical geometry[7], where the poloidal component of the k-space selection criterion reduces to $\langle m,m',m-m'\rangle$. This approximation is often retained for convenience, particularly when internal measurements are not available. In tokamak and reversed-field pinch (RFP) experiments that explore the combined effects of toroidal and 3-wave coupling on stability and plasma braking[6-10], however, it does not account for some observations[2,11].

It is well known that a single helicity, m/n, does not describe the global mode structure. In tokamak geometry, the *m*-number of either mode varies as a function of plasma radius away from the rational surface at which tearing occurs. Determining whether or not conditions for 3-wave coupling are met, therefore, requires internal diagnosis of the local wavenumber, as a function of plasma radius, for all three modes.

In this paper, ECE-Imaging data is analyzed to identify phase-locking and nonlinear coupling. Section 2 will discuss the approximation of 2D power spectral density from imaging diagnostic data. Phase velocities are evaluated near the midplane and at outboard radii, where coupling is strongest and modes are known to preferentially align x-point to x-point[12,13]. Phase-locking, the synchronous phase propagation of non-axisymmetric flux surface displacements (with either tearing or kinking parity), is identified in a range of DIII-D discharges. In Section 3, a typical case of coupling amongst $m/n=\langle4/3,3/2,2/1\rangle$ NTMs and the impact this coupling has on rotation and flow shear in the core is discussed. The prospect for advancing a theoretical description of these phenomena through new experimental techniques is discussed briefly in Section 4.

II. APPROXIMATION OF THE 2D POWER SPECTRAL DENSITY, $S(\omega,k_{pol})$

Fourier transformation of diagnostic signals in order to obtain the frequency spectrum of plasma oscillations, including higher order spectra such as the coherent bispectrum[14], is a routine practice. For arrays of fixed-point, localized measurements, one may also estimate the wavenumber spectrum[15]. Estimation of a 2D spectra, however, is non-trivial in the presence of turbulence, noise, and multiple, simultaneous modes, where a deterministic dispersion relation $k(\omega)$ does not exist. We apply a statistical method for estimating the 2D power spectrum developed by Beall, et. al.[16]. In keeping with the language and notation of that work, the conventional local wavenumber, $K(\omega)$, within a given time window *j*, is obtained by, $K^j(\omega)=\theta^j(\omega)/\Delta x$, where $\Delta x\equiv x_2-x_1$ is the separation between the measurements and $\theta(\omega)$ is obtained as the argument of the cross-spectrum, $\Phi^{j*}(x_1,\omega)\Phi^j(x_2,\omega)$. A 2D probability distribution function for the fluctuations, $p(K,\omega)$, is obtained by binning measurements from a set of time records, *M*, and all channel pairs (typically 20 local measurements at each plasma radius[17]) to divisions $K+\Delta K$. Normalizing each contribution to the power in that signal component results in a 2D power spectral density.

[a)]Contributed paper published as part of the Proceedings of the 20th Topical Conference on High-Temperature Plasma Diagnostics, Atlanta, Georgia, June, 2014.
[b)]Author to whom correspondence should be addressed: bjtobias@pppl.gov.

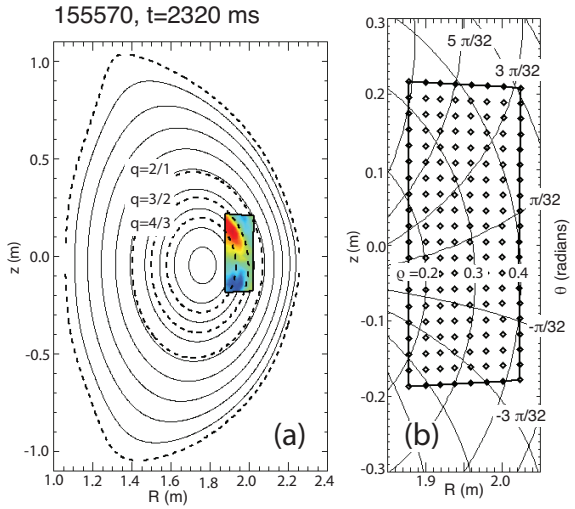

FIG. 1. (Color online). (a) An ECE-Image of the 3/2 mode overlaid on EFIT reconstruction of shot #155570. (b) The locations of individual ECE measurements are plotted along with contours of constant ρ and straight-field-line poloidal angle, θ. For this experiment, the ECE-Imaging array extends over approximately 0.3π radians of poloidal angle from ρ=0.2 to 0.4.

An upper bound on detectable wavenumber is set by the aliasing condition, $|k| < \pi/\Delta x$. Figure 1 shows the real-space locations of measurements made in shot #155570. Unique two-point measurements are made up to 1.5 cm^{-1} (anti-aliasing techniques beyond the scope of this paper are applied to pairs with larger separation). There is no ideal lower limit on the approximation of K. In practice, however, it is constrained by finite spatial resolution, imperfections in the alignment of the diagnostic, noise, and other sources of uncertainty in the cross-correlation phase, $\theta^j(\omega)$. The smallest discernable change in wavenumber for this experiment is $\Delta k_{pol} = 0.4$ m^{-1}, which is sufficiently small compared to the wavenumber of the $m/n = 2/1$ mode, $k_{pol} \simeq 2\pi$ m^{-1}.

A necessary condition for phase-locking is an agreement in phase velocity, $v_p = \omega/k$, amongst the modes. Axisymmetry ensures that the selection criterion $\langle k,k',k-k'\rangle_{toroidal}$ is equivalent to $\langle n,n',n-n'\rangle$. The poloidal wavenumber is measured along a selection of ECE-Imaging channels, and the poloidal phase velocity of an NTM in the laboratory frame is obtained directly from inspection of $S(\omega,k_{pol})$. Saturated, non-disruptive NTMs on DIII-D propagate in the ion diamagnetic direction with approximately 1 kHz of upshift with respect to the carbon impurity ion fluid rotation[18,19]. This offset is ignored for the present discussion as it is small compared to the Doppler shift and changes in rotation that are detailed in the next section.

III. ROTATION DAMPING DUE TO THE PHASE-LOCKING OF NTMs

Evolution of the fluid rotation for shot 155570 is shown in Figure 2. Early injection of co-I$_p$ tangential neutral beams produces a peaked toroidal rotation profile at the onset of a core 3/2 tearing mode. The continuing evolution of the high-confinement phase destabilizes a 2/1 island at t=2180 ms. In a series of similar discharges taken throughout the experiment, toroidal rotation is quickly damped inside the $q = 2$ surface, coincident with phase-locking of the rotating 3/2 and 2/1 perturbations. For reasons yet to be fully understood, this phase-locking evolves more slowly in shot #155570, culminating at t=2565 ms. After this time, 3-wave coupling selection criteria are satisfied amongst the 3/2, 2/1, and 4/3 NTMs. Once phase-locking is achieved, there are no cases of spontaneous unlocking; harmonics of the two branches are no longer distinct in $S(\omega,k_{pol})$ and the modes propagate with no more than 5 km/s differential velocity, despite the system being repeatedly perturbed by ELMs.

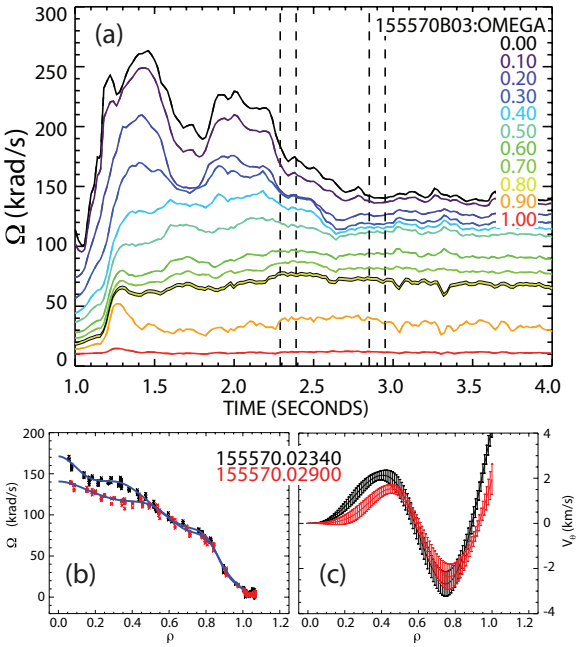

FIG. 2. (Color online). (a) Toroidal rotation as a function of time. 2/1 mode onset occurs at t=2180 ms, phase-locking at t=2565 ms. CER constrained fits of the toroidal (b) and poloidal (c) carbon impurity fluid rotation.

The dynamics of 3/2 and 2/1 mode coupling is presented in Figure 3. Beginning at t=2180 ms, the two modes rotate independently with a differential phase velocity (continuously oscillating relative phase). Nonetheless, nonlinear coupling is evident in analysis of the bicoherence[14,20]. Bicoherence indicates the presence of quadratic nonlinearities and phase coherence at $\omega = \omega_1 + \omega_2$. Unfortunately, the theory of 3-wave inter-mode coupling does not adequately describe the generation of electromagnetic torques at finite slip frequency, $\omega_s \equiv \Delta v_p/\Delta k$. This will be revisited in Section 4.

At t=2565 ms, the time of phase-locking, toroidal and poloidal selection criteria are satisfied in the region of imaging. Toroidal mode numbers $n = \langle 3,2,1\rangle$ constitute good quantum numbers and satisfy the toroidal selection criterion. However, the poloidal wavenumber criterion is met by islands of the set $m = \langle 4,3,2\rangle \neq \langle m,m',m-m'\rangle$. At the rational surface, the vertical, z-directed wavenumber of the island is $m\,d\theta/dz$. Although $d\theta/dz$ decreases with major radius, the local m-numbers one obtains by fitting the kink-like response on a flux surface increase[21]. The fluctuation associated with the 4/3 island fits well to $m = 5$ near the 2/1 surface, helping to locally satisfy $\langle m,m',m-m'\rangle$.

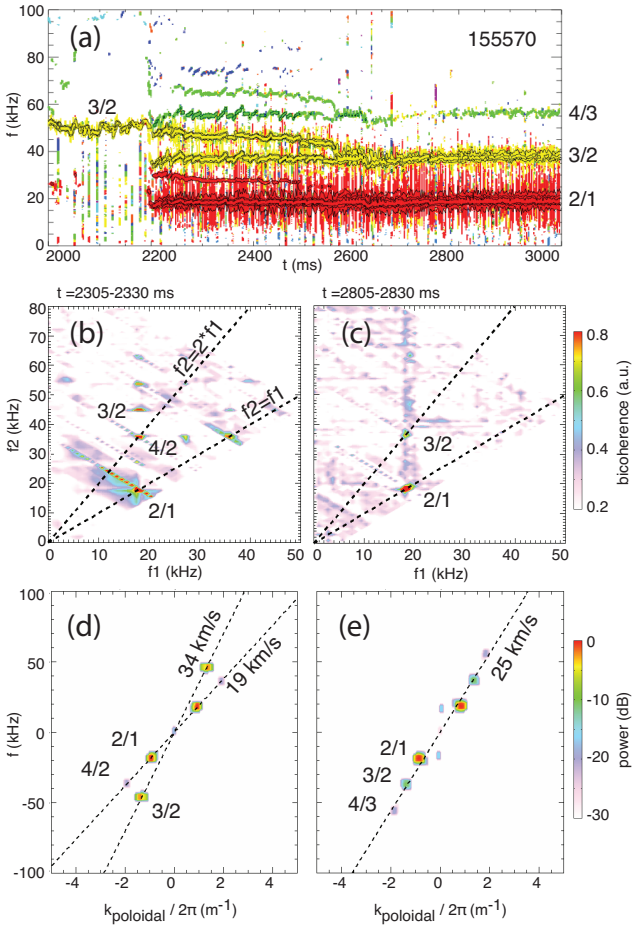

FIG. 3. (Color online). (a) A spectrogram of magnetic fluctuations. Coalescence of 3/2 and 4/2 island frequencies occurs near t=2580 ms. (b,c) Bicoherence estimates before and after phase-locking . (d,e) Local phase velocities near ρ=0.4, measured by ECE-Imaging.

At the first instance of phase-locking, there is a coalescence in $S(\omega,k_{pol})$ of the 3/2 mode and the $n=2$ harmonic of the 2/1 mode, $m/n=4/2$. The fluctuations associated with these modes evolve in order to satisfy the condition $\langle \omega=\omega', k=k' \rangle$ at all radii near the outboard midplane. This is phenomenologically distinct, however, from toroidal coupling[22,23] in that the 4/2 mode is stable in the absence of the 2/1 mode. The torque associated with this interaction is not separable from that which we attribute to nonlinear, 3-wave coupling. The mechanisms are inexorably intertwined. Therefore, the stability of self-harmonics must be treated self-consistently as an inherent aspect of 3-wave coupling theory, and vice versa. In the next section we discuss prospects for quantitatively validating a theory of this kind.

IV. FUTURE WORK

As nonlinear coupling proceeds, we also observe that the radial eigenfunction of each participating mode evolves. Future work will endeavor to make use of these differences between the linear and nonlinearly coupled eigenfunctions in order to approximate both the magnitude and distribution of mutual torques.

Nonlinear modification of the eigenfunctions and elevated bicoherence occur at significant slip frequency. As for the case of a single helicity mode interacting with an external magnetic perturbation, adoption of a model similar to that of an induction motor is appropriate[24]. The strength of the poloidal electromagnetic torque takes the form,

$$T_\theta \propto \frac{(\omega\tau_S)(r_1/r_2)^{2m}}{1+(\omega\tau_S)^2\left[1-(r_1/r_2)^{2m}\right]^2}, \qquad (1)$$

where τ_s represents an appropriately obtained 'layer time' at the rational surface. A minimum in the mutual torque exists at a critical frequency, along with bifurcations analogous to those observed during the locking (and unlocking) of an internal mode to an external error field[25,26].

V. ACKNOWLEDGEMENTS

This work was supported in part by the US Department of Energy under DE-AC02-09CH11466, DE-FG02-99ER54531, DE-SC0003913, and DE-FC02-04ER54698. We thank the DIII-D team for their support of these experiments. The authors would also like to thank Dr. Michio Okabayashi and Dr. George McKee for their generous contributions. DIII-D data shown in this paper can be obtained in digital format by following the links at https://fusion.gat.com/global/D3D_DMP.

VI. REFERENCES

[1]A. Gude *et al.*, Nuclear Fusion **39**, 127 (1999).
[2]M. Nave *et al.*, Nuclear Fusion **43**, 179 (2003).
[3]Q. Yu *et al.*, Nuclear Fusion **52**, 063020 (2012).
[4]J. Connor *et al.*, Physics of Fluids **31**, 577 (1988).
[5]R. Fitzpatrick *et al.*, Nuclear Fusion **33**, 1533 (1993).
[6]C. Hegna, Physics of Plasmas **3**, 4646 (1996).
[7]E. Lazzaro *et al.*, Physics of Plasmas **9**, 3906 (2002).
[8]R. Coelho *et al.*, Physics of Plasmas **6**, 1194 (1999).
[9]R. Fitzpatrick, and P. Zanca, Physics of Plasmas **9**, 2707 (2002).
[10]R. Coelho, E. Lazzaro, and P. Zanca, in *20th IAEA-FEC* (2005), pp. TH/P5.
[11]R. Buttery *et al.*, Nuclear Fusion **43**, 69 (2003).
[12]T. Hender *et al.*, Nuclear Fusion **44**, 788 (2004).
[13]B. Tobias *et al.*, Plasma Phys. and Control. Fusion **55**, 095006 (2013).
[14]Y. C. Kim, and E. J. Powers, Physics of Fluids **21**, 1452 (1978).
[15]N. Iwama, Y. Ohba, and T. Tsukishima, J. of Appl. Phys. **50**, 3197 (1979).
[16]J.M. Beall, Y.C. Kim, and E.J. Powers, J. of Appl. Phys. **53**, 3933 (1982).
[17]B. Tobias *et al.*, Rev. of Sci. Instrum. **81**, 10D928 (2010).
[18]R. La Haye *et al.*, Physics of Plasmas **10**, 3644 (2003).
[19]R. La Haye, Bull. of the American Physical Society **54** (2009).
[20]D. Raju, O. Sauter, and J. B. Lister, Plasma Phys. and Control. Fusion **45**, 369 (2003).
[21]B. Tobias *et al.*, Plasma Phys. and Control. Fusion **55**, 125009 (2013).
[22]M. Nave *et al.*, European Physical Journal D **8**, 287 (2000).
[23]B. Carreras, H. Hicks, and D. Lee, Phys. Fluids **24**, 66 (1981).
[24]R. Fitzpatrick, Nuclear Fusion **33**, 1049 (1993).
[25]D. Gates, and T. Hender, Nuclear Fusion **36**, 273 (1996).
[26]F. Waelbroeck, Nuclear Fusion **49**, 104025 (2009).

Princeton Plasma Physics Laboratory
Office of Reports and Publications

Managed by
Princeton University

under contract with the
U.S. Department of Energy
(DE-AC02-09CH11466)

P.O. Box 451, Princeton, NJ 08543
Phone: 609-243-2245
Fax: 609-243-2751

E-mail: publications@pppl.gov
Website: http://www.pppl.gov